Rapid Evolution of 6-Phenylpurine Inhibitors of Protein Kinase B through Structure-Based Design

Alastair Donald,[†] Tatiana McHardy,[†] Martin G. Rowlands,[†]
Lisa-Jane K. Hunter,[†] Thomas G. Davies,[‡] Valerio Berdini,[‡]
Robert G. Boyle,[‡] G. Wynne Aherne,[†]
Michelle D. Garrett,[†] and Ian Collins*[,†]

Cancer Research UK Centre for Cancer Therapeutics, The Institute of Cancer Research, 15 Cotswold Road, Sutton, Surrey, United Kingdom SM2 5NG, and Astex Therapeutics Ltd., 436 Cambridge Science Park, Milton Road, Cambridge, United Kingdom CB4 0QA

Received January 23, 2007

Abstract: 6-Phenylpurines were identified as novel, ATP-competitive inhibitors of protein kinase B (PKB/Akt) from a fragment-based screen and were rapidly progressed to potent compounds using iterative protein−ligand crystallography with a PKA−PKB chimeric protein. An elaborated lead compound showed cell growth inhibition and effects on cellular signaling pathways characteristic of PKB inhibition.

The PI3K−PKB−mTOR cascade is an important cellular signaling pathway that regulates cell growth and proliferation, cell survival, protein synthesis, glucose uptake, and glycogen metabolism.[1,2] Protein kinase B (PKB or Akt) has a pivotal position in the pathway and is a well-validated anticancer target.[3] PKB is downstream of the tumor suppressor PTEN, which is deleted in many tumor types.[4] Upstream receptor tyrosine kinases, the lipid kinase PI3K and PKB itself, particularly the β-isoform, are commonly amplified or mutated at the genetic level, overexpressed, or overactivated in human tumors.[1,4] Analogues of the natural product rapamycin, which inhibit the signaling pathway at the downstream level of mTOR, have shown efficacy in early clinical trials.[2] In preclinical studies, tumor growth reduction in animal models was observed with a dual PI3K/mTOR inhibitor,[5] and a recently reported ATP-competitive inhibitor of PKB.[6] There is, therefore, considerable interest in the discovery of new small molecule inhibitors of PKB kinase activity, which may act through competition with ATP or through interaction with regulatory domains in the protein.[7] Some classes of ATP-competitive inhibitors have been reported, including pyridines,[6,8] azapanes,[9] toxoflavins,[10] and isoquinoline-5-sulfonamides[11,12] such as **1**[11] (Chart 1). We show here the use of iterative protein−ligand crystallography and structure-based design to rapidly identify novel, potent 6-phenylpurine PKBβ inhibitors.

A virtual screen of approximately 300 000 available low molecular weight compounds[13] (<250 kDa) was carried out using the published PKBβ coordinates.[14] Selected virtual hits with promising predicted binding modes, particularly occupation of the adenine binding pocket, were validated through bioassay and crystallography with a PKA−PKB chimera.[15] The use of PKA[9a,11] or PKA−PKB chimeras[9b] as surrogates for PKB is well established and is successful due to the high sequence homology of PKA and PKB in the ATP binding site (ca. 80%). In this work, a chimera with three PKA → PKB mutations in the kinase active site of PKA was used, namely, Val123 → Ala, Val104 → Thr, and Leu173 → Met. A fourth mutation, Gln181

Chart 1

1 (CCT077373)   **2**
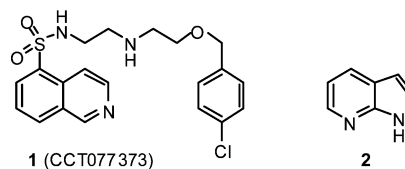
→ Lys, outside the ATP binding site, was made due to the potential for Gln181 to perturb ligand binding in the presence of the Val123 → Ala substitution.[15] We have recently shown that the binding modes of the unselective inhibitor **1** are identical in PKA, PKB, and the PKA−PKB chimera.[16] Additionally, for one PKB-selective inhibitor,[6] the chimera and PKB binding modes were similar, and distinct from the binding to PKA.[16] Although the use of PKB crystallography may be preferable for developing PKB selective ligands, the PKA−PKB chimera is suitable for guiding the de novo construction of inhibitor scaffolds.

7-Azaindole (**2** (pdb code 2UVX), Chart 1) was one fragment found to occupy the ATP-binding site, interacting through bidentate hydrogen bonding of the heterocyclic N and N−H to the backbone amides of Glu121 and Val123 (PKA−PKB chimera numbering) in the hinge region of the kinase (Figure 1a). Comparison with the crystallographic data[11] for **1** showed that this binding mode of **2** corresponded to the interactions of the isoquinoline nitrogen and adjacent C1-H. The other main determinants of binding for **1** to PKA and PKB are the basic amine, which interacts with acid side chains in the ribose binding pocket and the terminal lipophilic group that contacts the P-loop.[11]

We initially replaced the 7-azaindole with purine. This offered more flexible synthetic access to the required analogues, while potentially retaining the hydrogen bonding to the hinge region. A limited range of simple benzylamine and phenethylamine substituents were added to the purine core, aiming to access acidic residues in the ribose binding pocket. Suzuki couplings to the protected 6-chloropurine **3**[17] attached either benzaldehyde (**4**, **5**) or (cyanomethyl)phenyl (**8**, **9**) groups, which were elaborated by reductive amination and reduction, respectively (Scheme 1). The increase in PKBβ enzyme inhibition seen for compounds such as **6** (pdb code 2UVY), **7**, and **11** (Table 1) indicated that additional binding interactions were present, which was confirmed by crystallography with the chimera (Figure 1b). The ligand **6** occupied the ATP cleft, with bidentate hydrogen bonding of the purine mimicking the binding mode of **2**, as anticipated, and the basic nitrogen forming favorable electrostatic interactions with the acidic residue Glu127 and the backbone carbonyl of Glu170.[11] Several water molecules were also displaced by the 6-phenyl group relative to the structure of **2**. Compound **6** had good inhibitory activity for a small molecule, with a high ligand efficiency[18] ($\Delta g = 0.40$ kcal mol^{-1} per non-H atom), indicating an excellent start point for hit-to-lead evaluation. Unsurprisingly, **6** was equipotent against PKA (Table 1).

Comparison of the crystallographic data for **6** with that for **1** indicated that the benzylic position of the 4-benzylamine **6** provided a suitable attachment point for lipophilic substitution. This was achieved quickly through addition of Grignard reagents to the *N*-sulfinylimine[19] derived from the aldehyde **4** (Scheme 1). The resulting phenyl and benzyl substituted compounds **13**

---

* To whom correspondence should be addressed. Tel.: +44 2087224317. Fax: +44 02087224126. E-mail: ian.collins@icr.ac.uk.
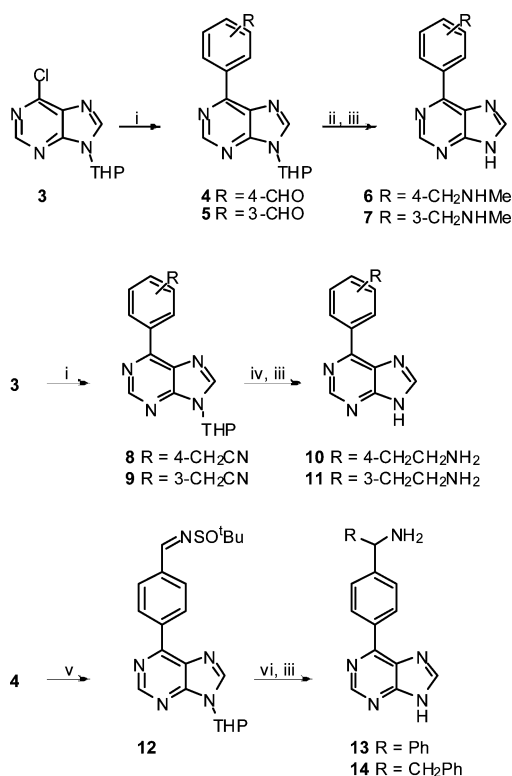† The Institute of Cancer Research.
‡ Astex Therapeutics Ltd.
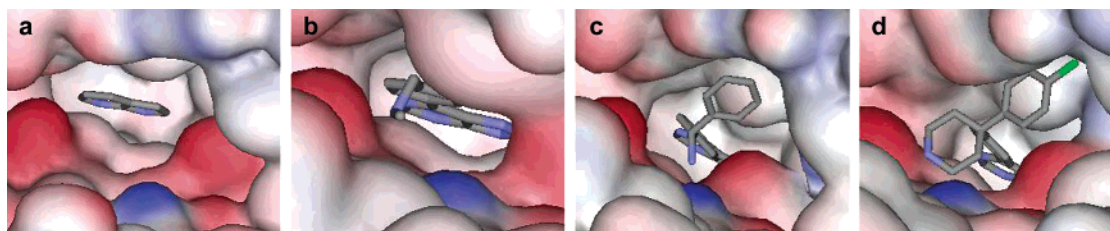
Figure 1. X-ray crystal structures of (a) **2**, (b) **6**, (c) **13**, and (d) **20** with PKA−PKB chimeric kinase domain. A detail of the ATP binding cleft is shown, oriented with the N-terminal domain and P-loop at the top of the panel, with the protein surface colored by electrostatic charge (red = negative, blue = positive, white = neutral). The prominent areas of negative charge are the side chains of Glu127 (left) and Asp184 (right).

Scheme 1[a]

[a] Reagents: (i) $ArB(OH)_2$, $Pd(PPh_3)_4$, K_2CO_3, DME; (ii) $MeNH_2$, EtOH, then $NaBH_4$, MeOH; (iii) HCl, EtOH; (iv) HCO_2NH_4, Pd/C, MeOH; (v) H_2NSO^tBu, PPTS, $MgSO_4$, CH_2Cl_2; (vi) RMgBr, $Et_2O−CH_2Cl_2$.

Table 1. Enzyme Inhibition, Cellular Growth Inhibition, and Calculated Physicochemical Properties of PKB Inhibitors

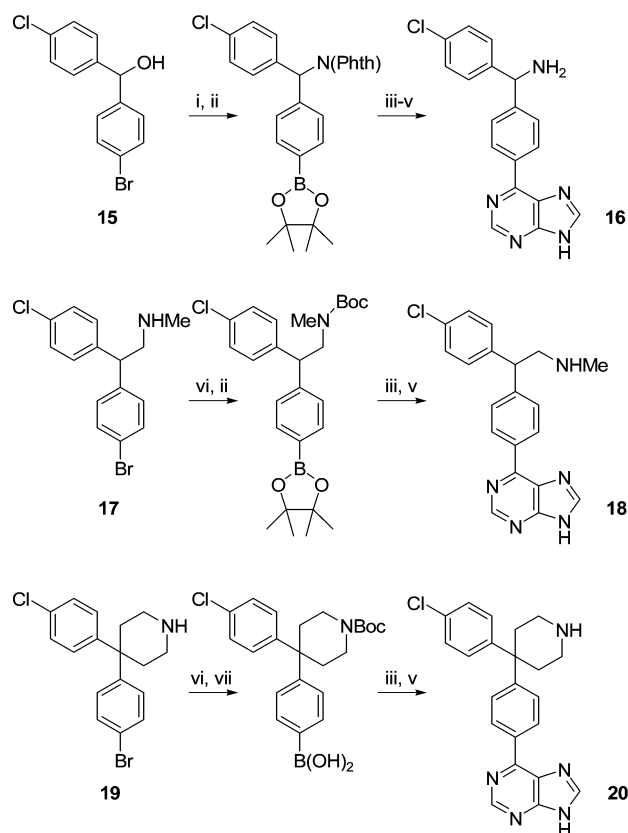| No.	PKBβ[a] IC$_{50}$ (μM)	PKA[b] IC$_{50}$ (μM)	PC3 SRB[c] GI$_{50}$ (μM)	ClogP	TPSA (A^2)
H-89	0.59 ($\pm$ 0.07)	0.073	18 ($\pm$ 1.4)	4.44	71
1	0.26 ($\pm$ 0.02)	0.17	25 ($\pm$ 1)	3.95	80
2	>100	n.d.[d]	n.d.	1.18	24
6	6.9 ($\pm$ 1.3)	5.2	>50	1.25	61
7	1.6 ($\pm$ 0.4)	5.5	>50	1.25	61
10	9.5 ($\pm$ 2.3)	n.d.	n.d.	1.17	75
11	3.2 ($\pm$ 0.4)	n.d.	>50	1.17	75
13	0.40 ($\pm$ 0.06)	n.d.	32	2.18	75
14	0.43 ($\pm$ 0.12)	0.61	32	2.71	75
16	0.009 ($\pm$ 0.003)	n.d.	28	2.89	75
18	0.010 ($\pm$ 0.003)	0.015	16	3.47	61
20	0.020 ($\pm$ 0.003)	0.033	4.5	4.81	61

[a] Inhibition of PKBβ kinase activity in a radiometric filter binding assay. Mean ($\pm$SEM) for $n = 3$ determinations. [b] Inhibition of PKA kinase activity in a radiometric filter binding assay. Single determinations from duplicate points. Standard isoquinoline-5-sulfonamide inhibitor H-8[11] gave IC$_{50}$ = 7.6 μM, SD $\pm$ 38% ($n = 14$) in this assay. [c] Cell growth inhibition (sulforhodamine B colorimetric assay) determined in PC3M prostate cancer cells. Mean of two independent determinations or mean ($\pm$SEM) for $n >$ 2 determinations. Standard isoquinoline-5-sulfonamide inhibitor H-89[11] gave SD $\pm$ 34% ($n = 20$) in this assay. [d] n.d. = not determined.

philic substituent was able to generate potent PKB inhibitors. However, compound **16** did not show an improvement in cell growth inhibition. Comparison of calculated values[20] for lipophilicity (ClogP) and polar surface area (TPSA) for the isoquinoline and purine inhibitors (Table 1) suggested that the purines had a lower ratio of lipophilicity to polar surface area, which we considered might impair cellular penetration. To probe this, we examined minor structural variations to **16** that increased the ratio of ClogP to TPSA.

Elaboration of the phenethylamine scaffold **17**[21] to prepare the *N*-methylated homologue **18** (Scheme 2) increased the lipophilicity somewhat and led to a 2-fold improvement in cellular activity. Compound **18** was prepared and tested as the racemate, and the individual enantiomers were not separated. We had previously observed[11] that there was some tolerance in the exact positioning of the basic amine in the ribose pocket with isoquinoline ligands, reflecting the possibility for productive binding interactions with either or both of the acid side chains Glu127 and Asp184, as seen for **6** versus **13** (Figure 1b,c and Figure 2a). Among other alterations to the inhibitor structures in the region of the basic amine, we prepared the 4-substituted piperidine **20** (pdb code 2UW0) from the bromide **19**[22] (Scheme 2). Compound **20**, which was substantially more lipophilic than **16** or **18**, maintained good enzyme inhibitory activity and ligand efficiency ($\Delta g = 0.38$ kcal mol^{-1} per non-H atom) and now showed much improved cell growth inhibition.

Comparison of the crystallographic data for **1** and **20** bound to the PKA−PKB chimera shows the close correspondence of the key pharmacophoric groups (Figure 2b). Several factors may explain the better PKB affinity of **20** relative to **1**. First, the hydrogen bonding to the hinge region of the kinase is supplied

(pdb code 2UVZ) and **14** showed a greater than 15-fold increase in PKB enzyme inhibition. The compounds were prepared and tested as racemates, although the crystal structure of **13** with the PKA−PKB chimera (Figure 1c) indicated that the *S*-enantiomer was binding preferentially. The position of the amine was observed to shift slightly relative to **6** and to make contacts with Asp184 and Asn171. The crystallographic data for **13** showed a change in the structure of the P-loop relative to that seen with **6**, such that the additional phenyl ring of **13** displaced the side chain of Phe54 and occupied the corresponding space. Potential for further substitution in this region was also evident. Importantly, cell growth inhibition, albeit weak, was now observed for **13** and **14**, which had similar profiles to the isoquinoline **1** (Table 1).

By analogy with the optimal 4-chlorophenyl group identified for **1**, 4-chloro substitution of **13** was investigated. A substituted arylboronate was constructed from the benzyl alcohol **15** before coupling to the 6-chloropurine **3** (Scheme 2). A further 40-fold increase in enzyme activity was observed, producing a nanomolar inhibitor of PKB, **16** (IC$_{50}$ = 9 nM). This confirmed that recapitulation of the 3-D pharmacophore defined by the bidentate hydrogen-bonding group, basic amine, and terminal lipo-

Scheme 2[a]

[a] Reagents: (i) phthalimide, DIAD, PPh$_3$, THF; (ii) bis(pinacolato)diboron, Pd$_2$(dba)$_3$, (*c*-hexyl)$_3$P, KOAc, dioxane; (iii) **3**, PdCl$_2$(PPh$_3$)$_2$, K$_2$CO$_3$, DME; (iv) NH$_2$NH$_2$, EtOH; (v) HCl−dioxane; (vi) (Boc)$_2$O, Et$_3$N, CH$_2$Cl$_2$; (vii) *n*-BuLi, B(O*i*-Pr)$_3$, THF.
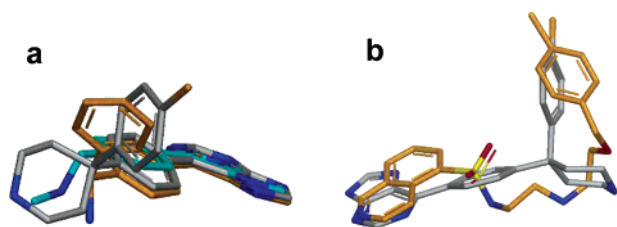
Figure 2. Overlay of bound conformations of (a) **6** (cyan), **13** (gold), and **20** (gray) and (b) **1** (gold) and **20** (gray), as determined by crystallography with PKA−PKB chimera.

by two overt hydrogen bonds for **20**, whereas one of these is a weaker C−H···O type interaction in **1**. Second, it is clear from the overlay that the more rigid structure **20** delivers the key functional groups to the protein's surface in a more efficient manner than **1**. In particular, more rotatable bonds must be frozen for the binding of **1**, leading to a higher entropic penalty, which would compromise the overall binding affinity. The enzyme inhibitory activity and binding mode of **20** was comparable to that of a related 4-phenylpyrazole discovered through parallel optimization of a pyrazole fragment hit.[23]

Compound **20** was examined for growth inhibition in other cell lines and showed a similar level of activity (Table 2). For some of these, the cellular mechanism of action of **20** was probed using a cellular ELISA protocol to examine phosphorylation of GSK3β, an immediate downstream substrate for PKB.[24] This quantification of the inhibitory potency of the compound in cells indicated that modulation of the target activity was occurring at similar concentrations to the cell growth inhibition. The difference between the enzymic inhibitory activity of **20** and the cellular activity may indicate that cell

Table 2. Growth Inhibition and Target Modulation in Cells by **20**

cell line	growth inhibition SRB[a] GI$_{50}$ (μM)	pGSK3β ELISA[b] IC$_{50}$ (μM)
PC3M (prostate)	4.5	6.0
HCT116 (colon)	5.7	n.d.[c]
U87MG (brain)	8.7 (± 0.5)	1.9 (± 0.7)

[a] See footnote to Table 1 for details of assay variability. [b] Single determination or mean (±SEM) for $n = 3$. Standard isoquinoline-5-sulfonamide inhibitor H-89[11] gave IC$_{50}$ 15 (± 2) μM in PC3M cells. [c] n.d. = not determined.
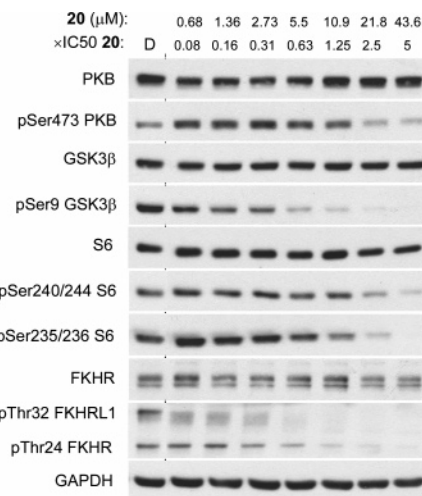
Figure 3. Western blot showing titration of the effect of compound **20** on the phosphorylation state of components of the PI3K−PKB−mTOR pathway in U87MG glioblastoma cells after 1 h treatment. D = DMSO control.

penetration is unoptimized for these compounds or may reflect the degree to which the pathway is sensitive to inhibition of PKB in these cell lines.

The effects of **20** on the PI3K−PKB−mTOR and associated pathways in U87MG glioblastoma cells was examined by Western blot using phospho-specific antibodies (Figure 3). This cell line has recently been shown to be particularly relevant for the characterization of inhibitors of the PI3K−PKB−mTOR pathway.[5]

At similar concentrations to the IC$_{50}$ for cell growth inhibition, compound **20** showed inhibition of signaling through PKB. Effects were seen in multiple branches of the downstream pathway, with decreases in the levels of pGSK3β, pS6, and pFKHR proteins. An increase in the levels of pSer473−PKB was observed at low concentrations of **20**, suggesting increased activation of PKB in response to pathway inhibition. This is consistent with the recently identified feedback inhibition pathway from activated p70S6K, downstream of PKB, to the upstream regulator IRS1.[5,25] Although the release of this feedback through inhibition of PKB may elicit a compensatory upregulation of signaling in the pathway, it is important to note that overall inhibition of downstream signaling, and cell growth, is seen with compounds such as **20**.

To further assess the potential of the 6-phenylpurine scaffold as a lead PKB inhibitor, the inhibitory effect of **20** on important cytochrome P450 isoforms in vitro was measured. Compound **20** showed IC$_{50}$ >10 μM for CYP1A2, CYP2C9, and CYP2D6, while some inhibition of CYP3A4 (IC$_{50}$ ∼ 10 μM) and CYP2C19 (IC$_{50}$ = 1.6 μM) was observed.

In summary, elaboration of the very low affinity fragment hit **2**, using iterative protein−ligand crystallography, allowed us to rapidly identify novel PKB inhibitors based on the

6-phenylpurine scaffold. The lead compound **20** shows potent enzyme inhibition, appropriate cellular activity, and has tractable physicochemical properties consistent with further optimization. The evolution of **2** to **16** and **20** shows how potent inhibitors of PKBβ can be derived from an understanding of the PKB/PKA pharmacophore. Selectivity for inhibition of PKB over PKA may be desirable, as PKA activity has been found to be both oncogenic and tumor-suppressing, dependent on cellular context.[26,27] To introduce this, it will be necessary to consider more closely the differences between PKB and PKA.[16]

Supporting Information Available: Experimental details for the preparation of **13**, **14**, **16**, **18**, and **20**, experimental details for pGSK3β ELISA and SRB cellular assays, and X-ray crystallography statistics (**2**, **6**, **13**, **20**). This material is available free of charge via the Internet at http://pubs.acs.org.

References

(1) Hennessy, B. T.; Smith, D. L.; Ram, P. T.; Lu, Y.; Mills, G. B. Exploiting the PI3K/AKT pathway for cancer drug discovery. *Nat. Rev. Drug Discovery* **2005**, *4*, 988–1004.

(2) Georgiakis, G. V.; Younes, A. From Rapa Nui to rapamycin: Targeting PI3K/Akt/mTOR for cancer therapy. *Expert Rev. Anticancer Ther.* **2006**, *6*, 131–140.

(3) Cheng, J. Q.; Lindsley, C. W.; Cheng, G. Z.; Yang, H.; Nicosia, S. V. The Akt/PKB pathway: Molecular target for cancer drug discovery. *Oncogene* **2005**, *24*, 7482–7492.

(4) Cully, M.; You, H.; Levine, A. J.; Mak, T. W. Beyond PTEN mutations: The PI3K pathway as an integrator of multiple inputs during tumorigenesis. *Nat. Rev. Cancer* **2006**, *6*, 184–192.

(5) Fan, Q. W.; Knight, Z. A.; Goldenberg, D. D.; Yu, W.; Mostov, K. E.; Stokoe, D.; Shokat, K. M.; Weiss, W. A. A dual PI3 kinase/mTOR inihibitor reveals emergent efficacy in glioma. *Cancer Cell* **2006**, *9*, 341–349.

(6) Luo, Y.; Shoemaker, A. R.; Liu, X.; Woods, K. W.; Thomas, S. A.; de Jong, R.; Han, E. K.; Li, T.; Stoll, V. S.; Powlas, J. A.; Oleksijew, A.; Mitten, M. J.; Shi, Y.; Guan, R.; McGonigal, T. P.; Klinghofer, V.; Johnson, E. F.; Leverson, J. D.; Bouska, J. J.; Mamo, M.; Smith, R. A.; Gramling-Evans, E. E.; Zinker, B. A.; Mika, A. K.; Nguyen, P. T.; Oltersdorf, T.; Rosenberg, S. H.; Li, Q.; Giranda, V. L. Potent and selective inhibitors of Akt kinases slow the progress of tumors in vivo. *Mol. Cancer Ther.* **2005**, *4*, 977–986.

(7) Barnett, S. F.; Bilodeau, M. T.; Lindsley, C. W. The Akt/PKB family of protein kinases: A review of small molecule inhibitors and progression towards target validation. *Curr. Top. Med. Chem.* **2005**, *5*, 109–125.

(8) Woods, K. W.; Fischer, J. P.; Claiborne, A.; Li, T.; Thomas, S. A.; Zhu, G.; Diebold, R. B.; Liu, X.; Shi, Y.; Klinghofer, V.; Han, E. K.; Guan, R.; Magnone, S. R.; Johnson, E. F.; Bouska, J. J.; Olson, A. M.; de Jong, R.; Oltersdorf, T.; Luo, Y.; Rosenberg, S. H.; Giranda, V. L.; Li, Q. Synthesis and SAR of indazole-pyridine based protein kinase B/Akt inhibitors. *Bioorg. Med. Chem.* **2006**, *14*, 6832–6846.

(9) (a) Breitenlechner, C. B.; Wegge, T.; Berillon, L.; Graul, K.; Marzenell, K.; Friebe, W. G.; Thomas, U.; Schumacher, R.; Huber, R.; Engh, R. A.; Masjost, B. Structure-based optimization of novel azepane derivatives as PKB inhibitors. *J. Med. Chem.* **2004**, *47*, 1375–1390. (b) Breitenlechner, C. B.; Friebe, W. G.; Brunet, E.; Werner, G.; Graul, K.; Thomas, U.; Kunkele, K. P.; Schafer, W.;

Gassel, M.; Bossemeyer, D.; Huber, R.; Engh, R. A.; Masjost, B. Design and crystal structures of protein kinase B-selective inhibitors in complex with protein kinase A and mutants. *J. Med. Chem.* **2005**, *48*, 163–170.

(10) Burns, S.; Travers, J.; Collins, I.; Rowlands, M. G.; Newbatt, Y.; Thompson, N.; Garrett, M. D.; Workman, P.; Aherne, G. W. Identification of small molecule inhibitors of protein kinase B (PKB) in an AlphaScreen high-throughput screen. *J. Biomol. Screening* **2006**, *11*, 822–827.

(11) Collins, I.; Caldwell, J.; Fonseca, T.; Donald, A.; Bavetsias, V.; Rowlands, M. G.; Hunter, L-J. K.; Garrett, M. D.; Davies, T. G.; Berdini, V.; Woodhead, S.; Davis, D.; Seavers, L. C. A.; Wyatt, P. G.; McDonald, E. Structure-based design of isoquinoline-5-sulfonamide inhibitors of protein kinase B. *Bioorg. Med. Chem.* **2006**, *14*, 1255–1273.

(12) Reuveni, H.; Livnah, N.; Geiger, T.; Klein, S.; Ohne, O.; Cohen, I.; Benhar, M.; Gellerman, G.; Levitski, A. Toward a PKB inhibitor: Modification of a selective PKA inhibitor by rational design. *Biochemistry* **2002**, *41*, 10304–10314.

(13) Rees, D. C.; Congreve, M.; Murray, C. W.; Carr, R. Fragment-based lead discovery. *Nat. Rev. Drug Discovery* **2004**, *8*, 660–672.

(14) Yang, J.; Cron, P.; Good, V. M.; Thompson, V.; Hemmings, B. A.; Barford, D. Crystal structure of an activated Akt/protein kinase B ternary complex with GSK3-peptide and AMP-PNP. *Nat. Struct. Biol.* **2002**, *9*, 940–944.

(15) Gassel, M.; Breitenlechner, C. B.; Ruger, P.; Jucknischke, U.; Schneider, T.; Huber, R.; Bossemeyer, D.; Engh, R. A. Mutants of protein kinase A that mimic the ATP-binding site of protein kinase B (AKT). *J. Mol. Biol.* **2003**, *329*, 1021–1034.

(16) Davies, T. G.; Verdonk, M. L.; Graham, B.; Saalau-Bethell, S.; Hamlett, C. C.; McHardy, T.; Collins, I.; Garrett, M. D.; Workman, P.; Woodhead, S. J.; Jhoti, H.; Barford, D. A structural comparison of inhibitor binding to PKB, PKA, and PKA–PKB chimera. *J. Mol. Biol.* **2007**, *367*, 882–894.

(17) Havelkova, M.; Hocek, M.; Cesnek, M.; Dvorak, D. The Suzuki–Miyaura cross-coupling reactions of 6-halopurines with boronic acids leading to 6-aryl- and 6-phenylpurines. *Synlett* **1999**, 1145–1147.

(18) Hopkins, A. L.; Groom, C. R.; Alex, A. Ligand efficiency: A useful metric for lead selection. *Drug Discovery Today* **2004**, *9*, 430–431.

(19) Liu, G.; Cogan, D. A.; Ellman, J. A. Catalytic asymmetric synthesis of *tert*-butanesulfinamide. Application to the asymmetric synthesis of amines. *J. Am. Chem. Soc.* **1997**, *119*, 9913–9914.

(20) ClogP and TPSA calculated using *ChemDraw Ultra 10.0*; CambridgeSoft: Cambridge, MA, 2007.

(21) Amschler, U.; Schultz, O. E. Halogen derivatives of epinephrine and isoproterenol. *Arzneim.-Forsch.* **1972**, *22*, 2095–2096.

(22) Berdini, V.; Boyle, R. G.; Saxty, G.; Verdonk, M. L.; Woodhead, S. J.; Wyatt, P. G.; Sore, H. F.; Caldwell, J.; Collins, I.; Da Fonseca, T. F.; Donald, A. PCT Intl. Pat. Appl. 046023; *Chem. Abstr.* **2006**, *144*, 450718.

(23) Saxty, G.; Woodhead, S. J.; Berdini, V.; Davies, T. G.; Verdonk, M. L.; Wyatt, P. G.; Boyle, R. G.; Barford, D.; Downham, R.; Garrett, M. D.; Carr, R. A. Identification of novel inhibitors of protein kinase B using fragment-based lead discovery. *J. Med. Chem.* **2007**, *50*, 2293–2296.

(24) Garrett, M. D.; Hunter, L. J.; Faria Da Fonseca, T.; Caldwell, J.; Rowlands, M. G.; Hardcastle, A.; Collins, I.; McDonald, E.; Thompson, N.; Workman, P. 322. Novel isoquinoline-5-sulfonamides as biochemical and cellular inhibitors of PKB/Akt. *Eur. J. Cancer Suppl.* **2004**, *2* (8), 98.

(25) Harrington, L. S.; Findlay, G. M.; Gray, A.; Tolkacheva, T.; Wigfield, S.; Rebholz, H.; Barnett, J.; Leslie, N. R.; Cheng, S.; Shepherd, P. R.; Gout, I.; Downes, C. P.; Lamb, R. F. The TSC1–2 tumor suppressor controls insulin–PI3K signaling via regulation of IRS proteins. *J. Cell Biol.* **2004**, *166*, 213–223.

(26) Bossis, I.; Stratakis, C. A. Minireview: PRKAR1A: Normal and abnormal functions. *Endocrinology* **2004**, *145*, 5452–5458.

(27) Bossis, I.; Voutetakis, A.; Bei, T.; Sandrini, F.; Griffin, K. J.; Stratakis, C. A. Protein kinase A and its role in human neoplasia: The Carney complex paradigm. *Endocr.-Relat. Cancer* **2004**, *11*, 265–280.